**An Ischemic Detection Method Based on Artificial Neural Networks from Electrocardiograms Using the Discrete Hermite Transform**

**Maiko Arichi**
Lincoln University

# 1 Introduction

Ischemic heart disease is one of the main common cause of death and an electrocardiogram (ECG) is used in the investigation of the heart disease. In this paper, detection of ischemia with the Discrete Hermite Transform (DHmT) will be done by a Neural Network. The Discrete Hermite Transform (DHmT) values can be used to detect the features of ischemic episodes, which are changes in the ST segment and the T wave.

## 1.1 ECG

An electrocardiogram (ECG/EKG) is an electrical impulse recording of the entire heart and is used for the investigation of heart disease. These impulses are recorded as a wave called P-QRS-T, as given in Figure 1. A wave represents an electrical event, such as atrial depolarization, atrial repolarization, ventricular depolarization, ventricular repolarization, or transmission through the His bundles, and so on [2].

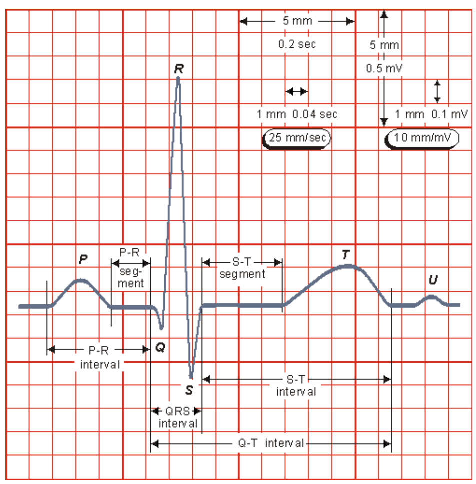


Figure 1: normal ECG signal [1]

# 2 Method

These methods concern the properties of the new set of digital Hermite functions as well as the application to ischemic detection. Detection of ischemia with the Discrete Hermite Transform (DHmT) will be done by a Nueral Network approach. In this approach, the DHmT values can be used to detect the features of ischemic episodes which are changes in the ST segment and the T wave. The method contains the following main steps as shown in Figure 2.

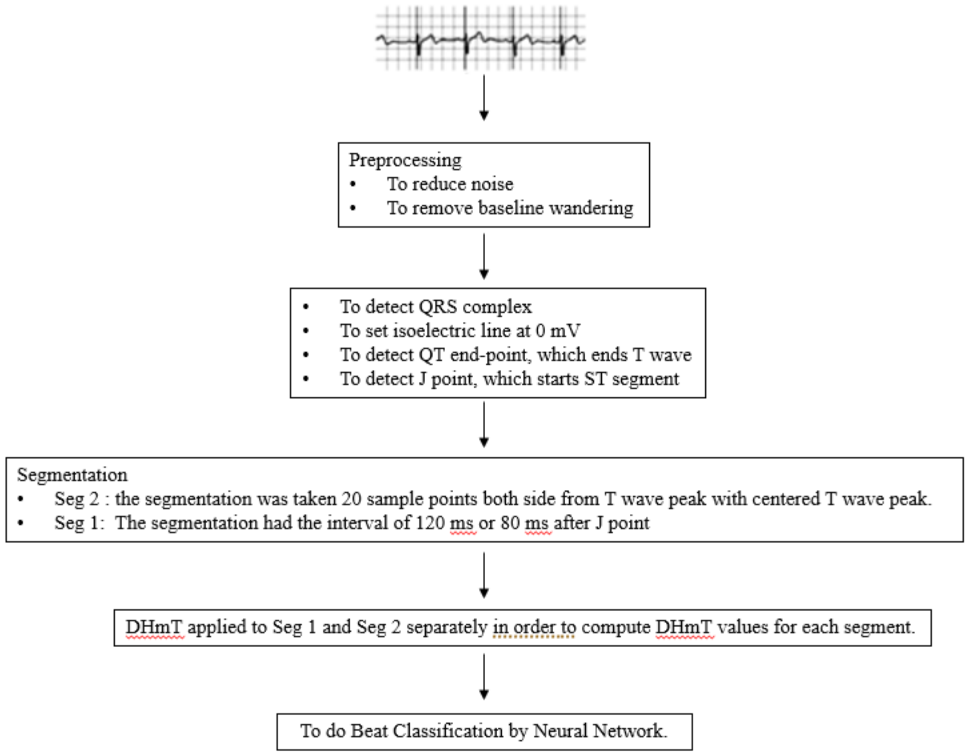


Figure 2: Neural Network Method

## 2.1 The Hermite Transform

**The Continuous Hermite Functions**. The classical Hermite functions are basically Hermite polynomials multiplied by the Gaussian function. The well-known form of the Hermite polynomials, using the Rodrigues Formula [11], are given by

$$P_{h,n}(t) = (-1)^n e^{t^2} \frac{d^n}{dt^n} e^{-t^2}, n = 0, 1, 2 \ldots, -\infty < t < \infty \tag{1}$$

The Hermite polynomials also satisfy many functional relations. They can be determined by the three-term recurrence relation [26]

$$P_{h,n+1}(t) = 2tP_{h,n}(t) - 2nP_{h,n-1}(t), n = 1, 2 \ldots \tag{2}$$

with initial conditions $P_{h,-1}(t) = 0$, $P_{h,0}(t) = 1$. The continuous Hermite functions, $h_n(t)$, $n \geq 0$, formed by the product of $e^{(-\frac{t^2}{2})}$ and a Hermite polynomial $P_{h,n}(t)$, have the property of being eigenfunctions of the continuous Fourier transform. In particular, the Fourier transform of $h_n(t)$ is $j^n$ times $h_n(t)$ where $j = \sqrt{-1}$ is the imaginary unit [12]. In addition, the initial Hermite function $h_n(t) = e^{(\frac{-t^2}{2})}$ is the Gaussian function.

**The Continuous Hermite Transform**. The Continuous Hermite Transform is the special case of the polynomial transforms in which the local window function $V(X)$ is Gaussian. The polynomial forward transform such as the polynomial coefficients $L_n(kT)$ has the following equation [24] [25];

$$L_n(kT) = \int_{-\infty}^{+\infty} L(x) \cdot G_n(x - kT)V^2(x - kT)dx \tag{3}$$

where $L(x)$ is the original signal, $G_n$ are the polynomials with degree $n$ that are orthonormal with respect to $V^2(x)$, $T$ is the period and $k$ is any integer. The polynomial inverse transform to reconstruct the original signal $L(x)$ has the following equation [24];

$$L(x) = \sum_{n=0}^{\infty} \sum_{k} L_n(kT) \cdot P_n(x - kT) \tag{4}$$

where the pattern function $P_n(x)$

$$P_n(x) = G_n(x)V(x)/W(x) \tag{5}$$

where the weight function $W(x)$ from the localized window function $V(x)$ is

$$W(x) = \sum_{k} V(x - kT) \tag{6}$$

In the polynomial transform, the coefficients $L_n(x)$ can be derived from the original signal $L_n(x)$ by convolving with the filter functions $D_n(x)$

$$D_n(x) = G_n(-x)V^2(-x) \tag{7}$$

The Continuous Hermite Transform has the Gaussian function as the local window function $V(x)$ in the polynomial transform.

$$V(x) = \frac{1}{\sqrt{\sqrt{\pi}}} exp(-x^2/2) \tag{8}$$

where the normalization factor is such that $V^2(x)$ has unit energy. The orthogonal polynomials that are associated with $V^2(x)$ are known as the Hermite polynomials $P_{h,n}(x)$. In the continuous Hermite Transform, the filter function $D_n(x)$ is known as the continuous Hermite function $h_n(x)$ [13] [24]

$$D_n(x) = h_n(x) = \frac{(-1)^n}{\sqrt{2^n n!}} \frac{1}{\sqrt{\pi}} P_{h,n}(x) e^{-x^2/2} \tag{9}$$

The continuous Hermite function $h_n(x)$ is equal to the $n$th order derivative of a Gaussian, therefore these filter functions can be interpreted very easily.

The $n$th Hermite coefficient with a original function $f(x)$ is defined by [26]

$$\hat{f}(n) = \int_{-\infty}^{\infty} f(x)\ h_n(x)dx \tag{10}$$

The reconstruction of the original function $f(x)$ using the inverse Hermite Transform is defined by

$$f(x) = \sum_{n=0}^{\infty} \hat{f}(n)\ h_n(x) \tag{11}$$

The shapes provided by the Hermite functions are appropriate in representing many biomedical signals, such as ECGs [27],[23]. The use of continuous Hermite functions in two-dimensional applications have been investigated for retinal vasculature [28].

**The Discrete Hermite Functions**. Mugler and Clary generated the discrete Hermite functions as eigenvectors of a symmetric tridiagonal matrix $T$ that commutes with the centered Fourier matrix $F_c$ [13]. This technique involves a symmetric tridiagonal matrix $T$ which has the same set of eigenvectors as the centered Fourier matrix $F_c$, which is a discrete analog for the continuous Fourier transform [11]. Since the matrix $T$ is symmetric, its eigenvectors are orthogonal and the vector set $h_0$, $h_1$,... $h_{n-1}$ is a set of vectors of length $n$ which forms a basis for $n$ dimensions. These eigenvectors satisfy the following property that they share with the continuous Hermite functions:

$$F_c \times h_k = j^k h_k \qquad\qquad k \in N \tag{12}$$

where $j = \sqrt{-1}$, $F_c$ represents the centered Fourier matrix and $h_k$ represents the discrete Hermite function. The property implies that a discrete Hermite function $h_k$ carries information about its frequency content since it is essentially its own Fourier transform. This discrete Hermite functions are approximately equal to uniformly sampled continuous Hermite functions $h_n(t)$ [13]. A complete basis of orthogonal digital signals $h_k$ for $0 \leq k \leq n-1$ have properties analogous to the continuous case. However, an attempt to form a set of digital signals by uniformly sampling the continuous Hermite functions $h_n(t)$ does not provide vectors that are mutually orthogonal [12].

**Dilated, Discrete Hermite Functions**. The set of eigenvectors of the tridiagonal matrix $T_\sigma$ are the dilated discrete Hermite functions $h_{k,\sigma}$. The continuous Hermite functions [11] are defined for $k \geq 0$ by

$$h_k(t) = e^{\frac{-t^2}{2}} P_{h,k}(t) \tag{13}$$

The continuous Hermite functions $h_k(t)$ are the Gaussian function multiple of a set of orthogonal polynomials. Therefore the dilated discrete Hermite functions $h_{k,\sigma}$ are similar to equation(13) with a dilation term $\sigma$; this set still retains orthonomality. The index $k$ stands for the number of zero crossings of the Hermite function in Figure 5. The effect of index $\sigma$ is that the function broadens with the value of $\sigma$ increasing and narrows down as its value decreases in Figure 3 and 4.

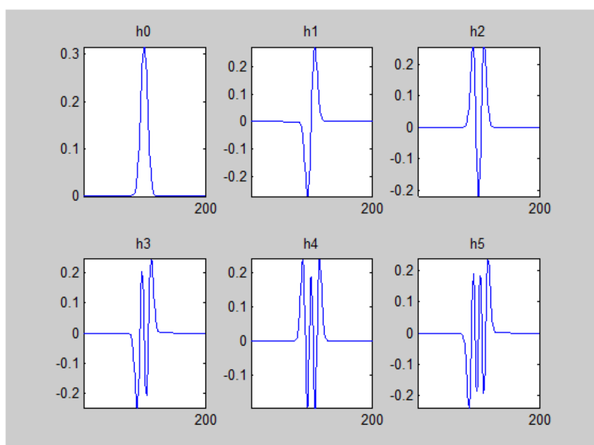


Figure 3: The first six undilated discrete Hermite functions $h_{k,\sigma}$ for $k = 0, 1...5$,$\sigma = 1$, $n = 200$

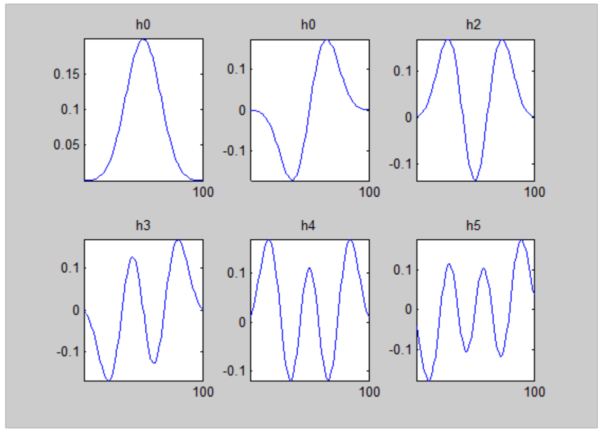


Figure 4: The first six discrete Hermite functions $h_{k,\sigma}$ for $k = 0, 1...5$,$\sigma = 3.5$,$N = 200$

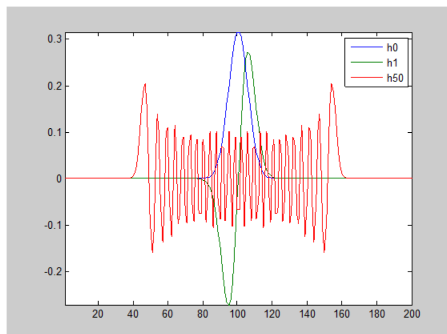


Figure 5: The undilated discrete Hermite functions $h_0, h_1$,and $h_{50}$, for $n = 200$

**The Discrete Hermite Transform (DHmT)**. The discrete Hermite transform (DHmT) is similar to the discrete Fourier transform, except that shapes instead of frequencies are the most important. The discrete Hermite transform of a digital input signal $x$ of length $N$ is simply the expansion of the digital signal in the orthonormal basis of dilated discrete Hermite functions [15] [18]. The Hermite transform of that signal provides a set of transform values which is computed by the inner product of the length $N$ input vector $x$ with the basis functions, just as the discrete Fourier transform is computed by an inner product with discrete complex exponentials. The basis functions for the DHmT have the additional property that they are essentially their own Fourier transform.

The Hermite transform of a digital input vector $x$ for dilation parameter $\sigma$, is given by

$$X_{H,\sigma}[k] = \langle x, h_{k,\sigma} \rangle = \sum_{n=0}^{N-1} x[n]\ h_{k,\sigma}[n] \tag{14}$$

for $k = 0, 1, 2, \ldots, N-1$. The input signal $x$ can be recovered without any error using the inverse discrete discrete Hermite transform whose formula is given by

$$x[k] = \sum_{j=0}^{N-1} X_{H,\sigma}[j]\ h_{k,\sigma}[j] \tag{15}$$

For example, if the discrete Hermite transform of an input signal $x$ is $x^H = [2, 3, -1, 0, \ldots 0]$, the function is $x = 2h_0 + 3h_1 - h_2$.The even-odd symmetry of the $h_{k,\sigma}$ functions allows for a relatively fast computation of the transform (or inverse transform), and current efforts concern a general fast computation method [16].

The application used by the discrete Hermite transform (DHmT) is a new technique and increasingly represented in digital form [15] [14] [17] [13] [12].

## 2.2 Fast Transform

**The Fast Fourier Transform (FFT)**. A Fast Fourier Transoform (FFT) is an efficient algorithm to compute the discrete Fourier Transform (DFT) and its inverse as well. FFTs were first discussed by Cooley and Tukey (1965), although Gauss had actually described the critical factorization step as early as 1805 (Bergland 1969, Strang 1993). The Cooley-Tukey algorithm is a much faster algorithm. The algorithm is to divide the transform into two pieces of size $N/2$ at each step, and is therefore limited to power-of-two sizes, but any factorization can be used in general. The most popular implementation of this algorithm is Radix-2 Cooley-Tukey. The computing time for the radix-2 FFT is proportional to $Nlog_2(N)$ rather than $N^2$ for DFT [19]. For example a transform on 1024 points using the DFT takes about 100 times longer than using the FFT. This shows the FFT is significantly better in speed.

## 2.3 Detection of Ischemic Heart Beats by using DHmT

**Ischemia**. Ischemic heart disease or ischemia is a condition in which fatty deposits accumulate in the cells of the coronary arteries [8]. These fatty deposits build up gradually and irregularly and encircle the heart and the main source of its blood supply, whose process is called atherosclerosis. This process leads to narrowing or hardening of the blood vessels supplying blood to the heart muscle. This causes an inability to provide adequate oxygen to the heart muscle and result in damage to it.

**Ischemic ECG waveforms**. Myocardial ischemia known as angina has three types, which are stable, unstable and variant. Stable myocardial angina occurs when the heart is working harder than usual and generally goes away with rest. Unstable myocardial ischemia is dangerous and requires emergency treatment. Variant myocardial ischemia occurs at rest and can be relieved by medicine.

Ischemia is a lack of sufficient oxygenated blood to the left ventricle and is manifested on the ECG by changes in the ST segment and T wave. Ischemia often causes ST segment depression with a sharp angle at the junction of the ST segment and T wave. Another commonly observed indication of ischemia is T wave inversion. Typically inverted (negative) T waves are relatively narrow and symmetrical [9].

The condition when the ischemic process is more severe is called injury. Subendocardial injury on a surface ECG is manifested by ST segment depression, and subepicardial or transmural injury is manifested as ST segment elevation [9]. Figure 6 shows the three criteria for Ischemia on the ECGs.

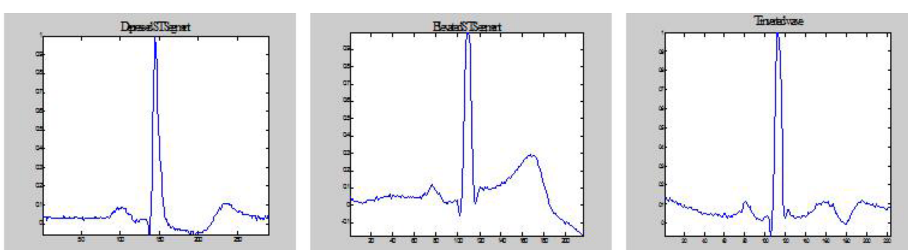

Figure 6: Abnormal ST segment and T wave in an ECG signal [3] [29]

## 2.4 Detection of isoelectric line

The preprocessing stage includes the noise reduction and removal of baseline wandering. For the noise reduction, a 4th order Butterworth low pass filter, with a cut off frequency of 40 Hz, is applied. For one cycle of a recorded cardiac beat, the first order polynomial of best fit is estimated. Baseline wandering is removed by subtraction of this polynomial from the recorded beat [6].

## 2.5 QRS complex and J point Dection

The R peak location is detected by using the Pan-Tompkins algorithm. The QRS complex has the largest slope in a cardiac cycle, by virtue of the rapid conduction and depolarization characteristics of the ventricles [30]. The S point is determined by finding the minimum value on the 50 ms interval after the R peak location. The Q point is determined by finding a minimum value on the 60 ms interval before the R peak location in a similar way. The determination of the S point and the Q point is done in a very similar way [31]. Figure 7 shows the QRS complex on a normal signal. The flat part of the ECG between the P wave and QRS complex is determined as the isoelectric line. The detection of an isoelectric line is the same as finding a zero-level reference point, denoted by $Z_0$. If the slope should be less than $Crit = 0.03(\max(\text{QRS})\text{-}\min(\text{QRS}))$ mV ms$^{-1}$ for an interval of 20 ms (5 sample points) for finding the flat interval $Z_0$, an average value of the voltage for these 5 sample points is calculated and the isoelectric line is set up at 0 mV by shifting signals upward or downward by the average value [32]. If the slope does not satisfy the above condition, then an interval of 16 ms (4 sample points) is used to find the slope that should be less than the critical value. The end of the T wave which is the right hand point in the T wave segment is determined by estimating the QT interval, called the QT segment. The QT segment depends on the RR interval.

$$QT = 0.4(\text{RR interval})^{1/2} * 250(\text{samples}). \tag{16}$$

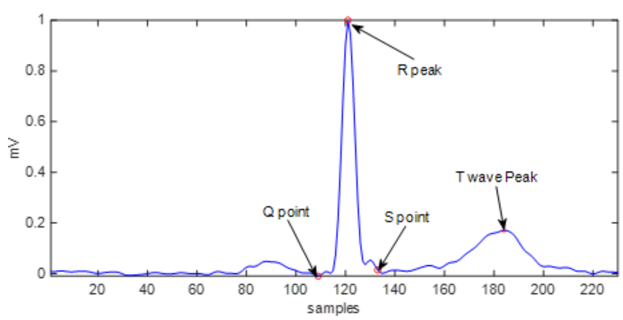


Figure 7: QRS complex on a normal signal (e0103)

The J point is a point at which the QRS complex meets the ST segment and the angle change occurs at this juncture [31]. The angle change means that the steep slope changes into a gentle slope at the J point. To find the J point, first the J-range between 4 ms and 60 ms after the S point is set. Second the slope over the J-range is calibrated. The J point is a point whose slope is less than 0.002 mV/ms, which means a flat slope. If this condition does not match, the J point is a point which is 16 ms after the S point location [31]. Figure 8 shows the J point location on the ECG signal.

There are two segmentations, Seg 1 and Seg 2, on an ECG signal in Figure 8. Seg 1 is used for detecting the ST elevation or depression, and Seg 2 is used for detecting the T wave changes. The Seg 1 is a segment that begins with the J point (the usual location of the beginning of the ST segment) and extends 30 sample points (120 ms) from the J point. If the heart rate is greater than 120 bpm, this is adjusted to 20 sample points (80 ms) so that segment does not include the T wave segment. Seg 2 is a

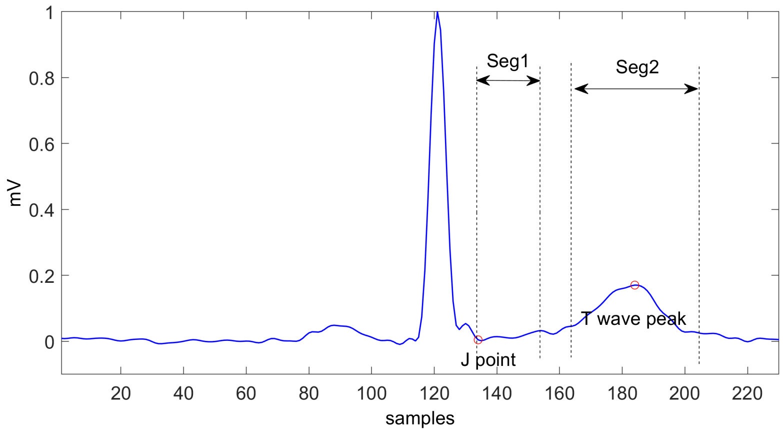


Figure 8: Seg 1 and Seg 2

segment taken 20 sample points (80 ms) from the T wave peak on both sides. This assumes a standard sampling rate of 250 Hz, as in the MIT-BIT database.

## 2.6 DHmT over Seg 1 and Seg 2

Figure 9 (a) shows a Seg 1 with a normal ST segment. The DHmT with $\sigma = 3.0$ is applied to the Seg 1 to get the DHmT values as given in Figure 9 (b). Figure 10 (a) shows Seg 1 with a ST depression. The corresponding DHmT values are given in Figure 10 (b). The Figure 11 (a) shows a Seg 1 with a ST elevation. The associated DHmT values are given in Figure 11 (b). The DHmT with $\sigma = 1.0$ is applied to the Seg 2 and $\sigma = 3.0$ is used for Seg 1. The DHmT values are given by the standard inner products of the input ECG signal with the dilated discrete Hermite functions.

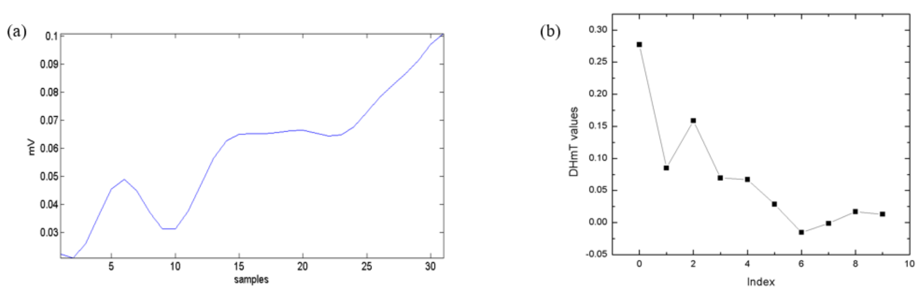


Figure 9: (a) Seg 1 with a normal ST segment (e0107), (b) The first 10 DHmT values of Seg 1 with a normal ST segment in (a)

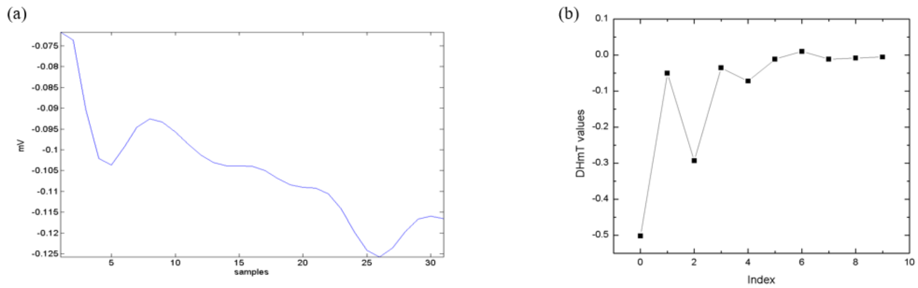


Figure 10: (a) Seg 1 with a ST depression (e0107), (b) The first 10 DHmT values of Seg 1 with a ST depression in (a)

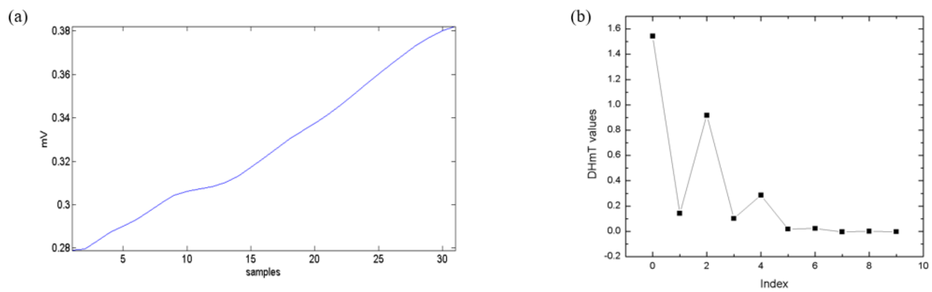


Figure 11: (a) Seg 1 with a ST elevation (e0104), (b) The first 10 DHmT values of Seg 1 with a ST elevation in (a)

The DHmT with $\sigma = 1.0$ is applied to the Seg 2 (the T wave peak centered segment) in order to get the DHmT values. The DHmT was applied to the Seg 2 with a normal T wave in Figure 12 (a) in order to get the DHmT values as given in Figure 12 (b). The DHmT was applied to the Seg 2 with an inverted T wave in Figure 13 (a) in order to get the DHmT values as given in Figure 13 (b).

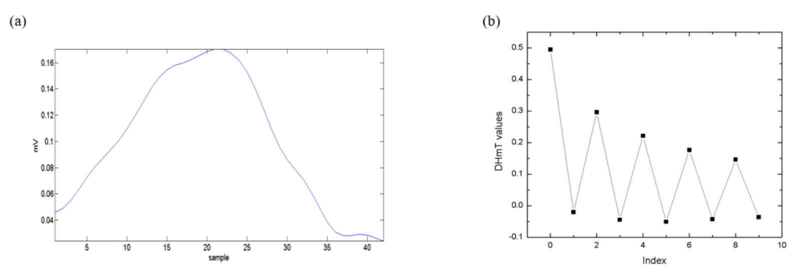


Figure 12: (a) Seg 2 with a normal T wave (e0103), (b) The first 10 DHmT values of Seg 2 with a normal T wave in (a)

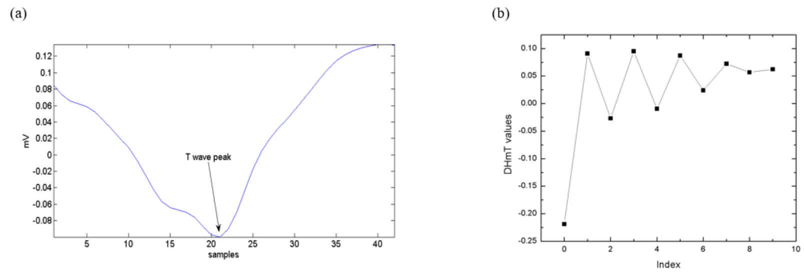


Figure 13: (a) Seg 2 with a T wave inversion (e0104), (b) The first 10 DHmT values of Seg 2 with a T wave inversion in (a)

### 2.7 Artificail Neural Network

The brain has the ability to perform tasks such as pattern recognition, perception and motor control much faster than any computer - even though events occur in the nanosecond range for silicon gates and milliseconds for neural systems. An artificial neural network(NN) is a model of biological neural systems that contains similar characteristics [33].

**Biological Neural System** A biological Neural System is comprised of a mass of nerve cells, referred to as a neuron. A neuron consists of a cell body, dendrites and an axon. Neurons are massively interconnected by interconnections between the axon of one neuron and a dendrite of another neuron. This connection is found in the synapse. Signals propagate from the dendrites, through the cell body to the axon,once the signal reaches to a synapse, these signals are propagated to all connected dendrites. A signal is transmitted to the axon of a neuron only when the cell undergoes depolarization and repolarization. A neuron can either inhibit or excite the associated post-symptic neurons.[33].

**Artificial Neuron (AN)** An artificial neuron (AN) is a model of a biological neuron (BN). Each AN receives signals from the environment or other ANs, and gathers these signals. When the cell is activated, each AN transmits a signal to all connected ANs. Figure 9 represents an artificial neuron (AN). Input signals are inhibited or excited through negative and positive numerical weights associated with each connection in the AN. The firing of an AN and the strength of the exciting signal are controlled via a function, called an activation function. The AN collects all incoming signals, and computes a net input signal using the respective weights, then the net signal serves as input to the activation function which calculates the output signal of the AN.

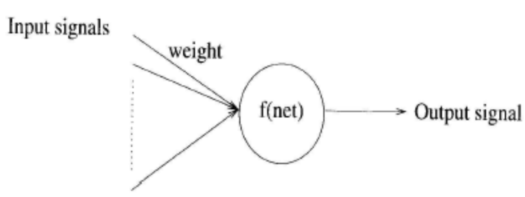


Figure 14: an artificial neuron [33]

**Basic Structure of an Artificial Network** An artificial neural network (NN) is a layered network of ANs. An NN consists of an input layer, one or more hidden layers and an output layer. ANs in one layer are connected, fully or partially, to the ANs in the next layer. A typical NN structure is represented in Figure 15.

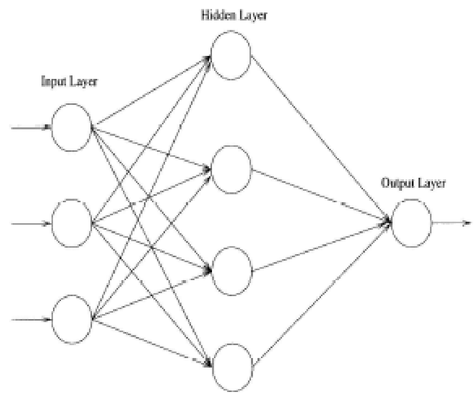


Figure 15: an artificial neural network [33]

The way to calculate the Net input signal is usually computed as the weighted ($w_i$) sum of all input signals ($x_i$) in Equation 17. These artificial neurons are referred to as *summation units* (SU) [33].

$$Net = \sum_i (x_i w_i) \tag{17}$$

Once the net input signal is calculated, the function $f_{Net}$, refereed to as the *activation function*, receives it to determine the output of the neuron. Different types of activation functions can be used.

The neural network is trained by a set of input data and the desired output, called targets using the back propagation algorithm. The back propagation algorithm, the best known training algorithm for the neural networks, is one in which the input data is continuously fed into the network and the predicted output of the network is compared with the desired output and the error generated. This process is done repeatedly until the error becomes insignificant.

The artificial neuron learning techniques are mainly classified into supervised and unsupervised learning, and the back propagation method is a type of supervised learning [33].

- **Supervised learning**, where the neuron (or NN) is provided with a data set consisting of input vectors and a target(desired output) associated with each input vector. This data set is referred to as the training set. The aim of supervised training is then to adjust the weight values such that the error between the real output of the neuron and the target output is minimized.

- **Unsupervised learning**, where the aim is to discover patterns or features in the input data with no assistance from an external source.

An artificial network has been used for a wide range of applications, including diagnosis of diseases, speech recognition, data mining, composing music, image processing, forecasting, robot control, credit approval, classification, pattern recognition, planning game strategies, compression and many others [33].

## 2.8 Ambiguous Annotation

There are some ambiguous annotations from the MIT-BIH database. For example, One patient $e0104$ from the MIT-BIH database has several ambiguous annotations. Figure 16 is the one of these ambiguous annotation examples. The annotation from the MIT-BIH database records these signals as normal signals, however, after time 26:25, these signals have T inverted waves. At the beginning of the records until time 26:25 in Figure 16, these signals have normal T waves, since the T wave is upright with an upright R wave, round and slightly assymetrical with more gradual slope on the first half of the wave than the second half of the wave. However, after time 26:25, each T wave at these signals is inverted after each ST segment, which means that these signals have abnormal T waves.

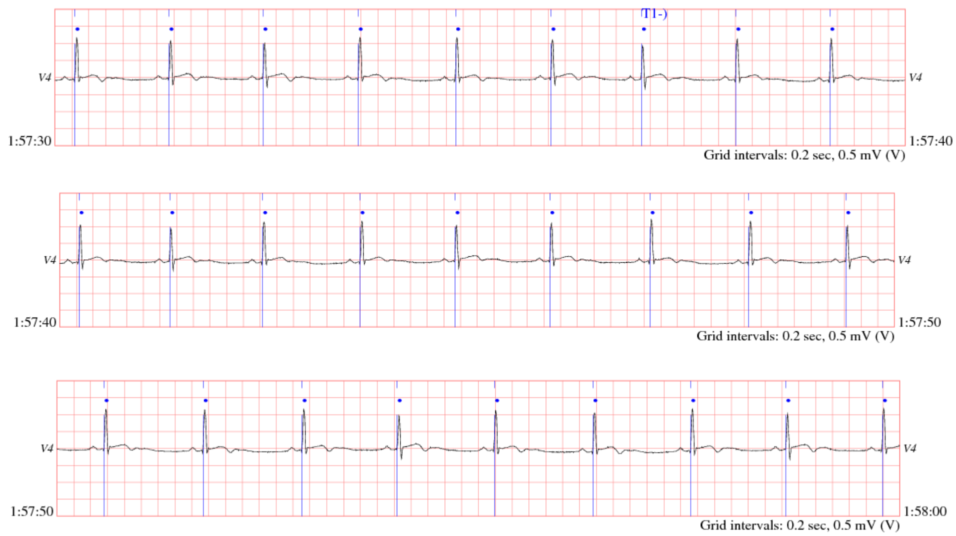


Figure 16: Inverted T waves can be seen, even though the annotation says normal signals. The recording time is 1:57:30 to 1:58:00. (e0104)

# 3 The ECG classification

In order to find out the usability of Hermite coefficients to identify ischemic features and their ability to classify each ECG signal as non-ischemic or ischemic, a committee Neural Network classifier is developed.

## 3.1 Training of a committee of Neural Networks

Five Neural Networks are developed and trained. Each network has three layers; input layer, hidden layer and output layer using feed forward network. The input layer has 50 neurons. The hidden layer has 35 to 55 neurons. The output layer has 3 neurons. The first 50 coefficients from the expansion of an ECG signal in discrete Hermite functions are used as input to the Neural Network. The outputs of the Neural Network are the presence/absence of ST-segment changes, the presence/absence of T-wave inversion and the presence/absence of ischemic ECG. Thus the targets should be the actual presence/absence of the ST-segment changes, T wave inversion and ischemic ECG. In both the hidden layer and the output layer, a tan-sigmoid function is used as the activation function. The conjugate gradient back propagation algorithm is used to train the network. ('trainscg' in the MATLAB Neural Network)

The individual network results might vary in borderline ischemic cases, so the majority decision of the committee of trained neural network is used for the final classification.

## 3.2 Testing network

A total of 24 long term ECG records from the European ST-T database, and the normal and ischemic episodes from the long term ST database were chosen to test the network, provided from the database.

- **Beat classification** is based on whether the network is able to detect any ST segment changes and T wave changes in a particular beat.

- **Episode classification** is based on whether a particular episode is rightly classified as ischemic or non-ischemic, irrelevant to the prediction of ST-segment and T-wave change.

## 3.3 Simulated Real-time model

A Hermite expansion that helps ECG segment classification is developed under the simulated real-time conditions for long term ECG monitoring applications. Figure 4.6 shows a simulated real time model of Hermite function based ischemic monitor for long term ECG signals.

The long-term ECG signals are scanned continuously for R-peak location using a QRS detection algorithm, *i.e.* the Pan-Tompkins algorithm. R-peak locations are used to automatically segment the ECG signal centered at its R-peak with a window size equivalent to the corresponding R-R interval. The individual ECG complexes are used to get the Hermite coefficients simultaneously using a simple dot product between the signal and the Hermite matrix using all coefficients.

The first 50 coefficients out of the generated ones are used as input to the trained Neural Network classifier. The network output has three, which are the presence/absence of ST-segment charge, the presence/absence of T-wave inversion and the presence/absence of ischemic ECG signal.

## 3.4 Testing

The network is tested with 24 long term ECG records as mentioned earlier. In addition to having been trained earlier, the Neural Networks are re-trained with a few initial samples of ECG cycles from each long term record that is used for testing in the simulated real-time model. This process shows the network a feel of the ST-segment and T-wave features from the particular long term ECG record and to find out if the network is able to detect any changes in the ST and T wave features that occurred during ischemic episodes.

## 3.5 Analysis for the performance

The method is evaluated by calculating the sensitivity, specificity and positive predictive value. These values give the accuracy of the method which is to determine how well a test can classify the diseased and the non-diseased, which is called a diagnostic test. Diagnostic test results have the following 4 possible choices:

- True-positive result, where the test is positive and patient has the disease.
- False-positive result, where the test is positive and patient does not have the disease.
- True-negative result, where the test is negative and patient does not have the disease.
- False-negative result, where the test is negative and patient has the disease.

The sensitivity, specificity and positive predictive values are calculated based on these four results. Here are the formulas.

$$Sensitivity = \frac{TP}{TP + FN} \tag{18}$$

$$Specificity = \frac{TN}{FP + TN} \tag{19}$$

$$Positivepredictivevalue = \frac{TP}{TP + FP} \tag{20}$$

Table 1: Performance analysis calculation of specificity, sensitivity and positive predictive value.

| TEST RESULT | DISEASE STATUS | |
|---|---|---|
| | **Present** | **Absent** |
| Positive | **True Positive (TP)** | **False Positive (FP)** |
| Negative | **False Negative (FN)** | **True Negative(TN)** |
| | **(TP + FN)** | **(FP + TN)** |

# 4 Results

## 4.1 DHmT over Seg2 (the T wave peak centered segment)

The Discrete Hermite Transform (DHmT) with $\sigma = 1.0$ is applied to the Seg2 in order to get the Discrete Hermite Transform values (DHmT values). The Discrete Hermite Transform values are used for the beat classification. Figure 17 (a) shows the Discrete Hermite Transform values for ten samples of Seg2 with normal T waves and Figure 17 (b) shows values for 10 samples of Seg2 with T inversion.

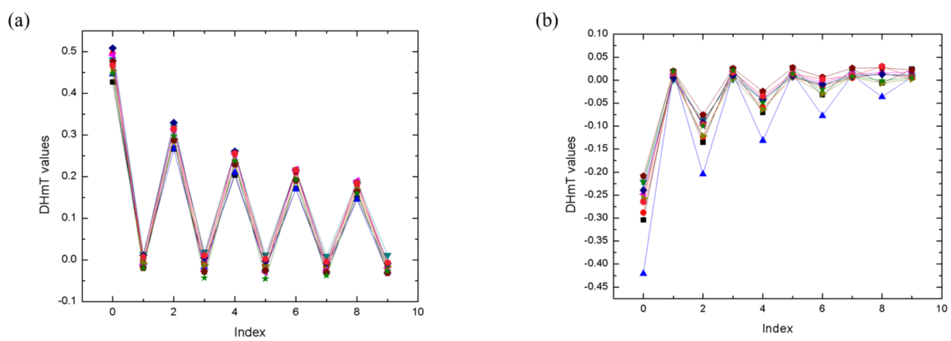


Figure 17: (a) The first 10 DHmT values for ten samples of a Seg 2 with normal T wave segment, (b) The first 10 DHmT values for ten samples of a Seg 2 with T inversion

## 4.2 DHmT over Seg1 (the segment for the ST elevation or depression determination)

The Discrete Hermite Transform (DHmT) with $\sigma = 3.0$ is applied to the Seg1 in order to get the Discrete Hermite Transform values (DHmT values). Figure 18 shows the first ten Discrete Hermite Transform values for five samples of Seg1 with the ST elevation and five samples of Seg1 with the normal ST segment. Both the first and third Discrete Hermite Transform values for Seg1 with the ST elevation are greater than ones for Seg1 with the normal ST segment.

Next classification is for the ST depression. Figure 19 shows the first 10 Discrete Hermite Transform values for five samples of Seg1 with ST depression and five samples of Seg1 with normal ST segments. The first and third Discrete Hermite Transform values of the Seg1 with the ST depression are less than the values of Seg1 with the normal ST segments.

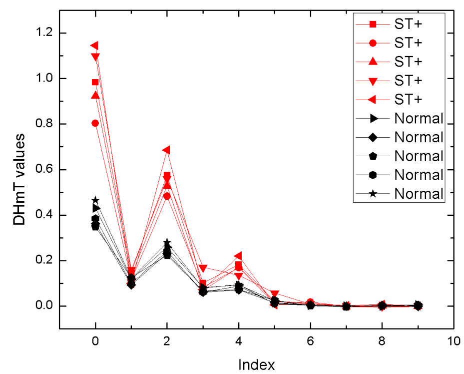


Figure 18: The first 10 DHmT values for five samples of Seg1 with ST elevation and normal

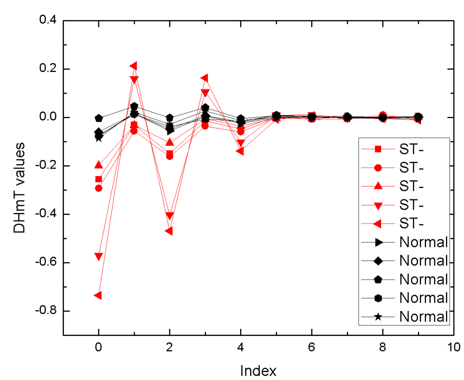


Figure 19: The first 10 DHmT values for five samples of Seg1 with ST depression and normal

### 4.3 Preliminary results

# 5 Results from ECG classification

Using the feature extraction capability of the Hermite coefficients classifies the beats into ischemic or not. A total 24 of long term ECG records are used to test the method, which contained 215 beats of which 93 are non-ischemic and 122 are ischemic.

The results of beat classification are tabulated in Table 2, 3 and 4. For ST segment changes (Seg 1), a sensitivity of 82.05 % and a specificity of 71.18 % are observed. For T-wave changes (Seg 2), a sensitivity of 85.22 % and a specificity of 46.15 % are observed. The positive predictive value of 88.27 % for ST-segment changes and of 88.23 % for T-wave changes are observed. Overall, for ischemic episode detection, a sensitivity of 72.72 % and a specificity of 68.67 % and a positive predictive value of 78.58 % are observed.

Table 2: Results for beat classification

| TEST RESULT | ST segment change(number of samples) | |
|---|---|---|
| | **Present** | **Absent** |
| Positive | **128** | **17** |
| Negative | **28** | **42** |
| | **156** | **59** |

$$\text{Sensitivity: } \frac{128}{156} \times 100 = 82.05\ \%$$

$$\text{Specificity: } \frac{42}{59} \times 100 = 71.18\ \%$$

$$\text{Positive predictive value: } \frac{128}{145} \times 100 = 71.18\ \%$$

Table 3: Results for beat classification

| TEST RESULT | T wave change(number of samples) | |
|---|---|---|
| | **Present** | **Absent** |
| Positive | **150** | **21** |
| Negative | **26** | **18** |
| | **176** | **39** |

Sensitivity: $\frac{150}{176} \times 100 = 88.23$ %

Specificity: $\frac{18}{39} \times 100 = 46.15$ %

Positive predictive value: $\frac{150}{171} \times 100 = 88.23$ %

Table 4: Results for beat classification

| TEST RESULT | ISCHEMIC (number of samples) | |
|---|---|---|
| | **Present** | **Absent** |
| Positive | **96** | **26** |
| Negative | **36** | **57** |
| | **132** | **83** |

Sensitivity: $\frac{96}{132} \times 100 = 72.72$ %

Specificity: $\frac{57}{83} \times 100 = 68.67$ %

Positive predictive value: $\frac{96}{122} \times 100 = 78.68$ %

# References


[1] J.Malmivuo AND R.Plonsey, *Bioelectromagnetism: Principles and Applications of Bioelectric and Biomagnetic Fields*, New York, Oxford, Chap.15,pp. 277-289.

[2] T.Garcia,B AND N.Holtz,*12-Lead ECG The Art of Interpretation*, Jones and Bartlett Publishers,Inc.,2001

[3] C.Papaloukas, D.I.Fotiadis, A.Likas, C.S.Stoumbis and L.K.Michalis, *Use of a Novel Rule-based Expert System in the Detection of Changes in the ST Segment and the T*, Journal of Electrocardiology, Vol 45, No.1, pp27-34, 2002.

[4] C.Papaloukas, D.I.Fotiadis, A.Likas, AND L.K.Michalis, *An expert system for ischemia detection based on parametric modeling and artificial neural networks*, Proc. Eur.Med.Biol.Eng.Conf., 2002, pp.742-743.

[5] C.Papaloukas, D.I.Fotiadis, A.Liavas, A.Likas, and L.K.Michalis, *A knowledge-based technique for automated detection of ischemic episodes in long duration electrocardiograms*, Med.Biol.Eng.Comput.,vol.39, 2001, pp.105-112.

[6] C.Papaloukas, D.I.Fotiadis, A.Likas, and L.K.Michalis, *An ischemia detection method based on artificial neural networks*, Artif.Intell.Med.,vol.24, 2002, pp. 167-178.

[7] M.Fassler,D AND B.Steuble.T, *Electrocardiogram Interpretation and Emergency Intervention*,Springhouse Corporation,1991

[8] D.Davis, *How to Quickly and Accurately Master ECG Interpretation*, J.B.Lippincott Company, Second Ed., 1992.

[9] Z.Abedin, *12 Lead ECG Interpretation: The Self-Assessment Approach*, W.B.Saunders Company, 1989

[10] J.Catalano,T, *Guide to ECG Analysis*, Lippincott Williams and Wilkins,2001,pp.241-243.

[11] A.D.Poularikas, *The Handbook of Formulas and Tables for Signal Processing*, CRC press Publ., Chap.22, pp.221-225.

[12] A.Mahadevan, S.Acharya, D.B.Sheffer and D.H.Mugler, *Ballistocardiogram Artifact Removal in EEG-fMRI Signals Using Discrete Hermite Transforms*, IEEE Journal of Selected Topics in Signal Processing, (2)6, December, 2008, pp. 839-853.

[13] D.H.Mugler, S.Clary and Y.Wu, *Discrete Hermite Expansion of Digital Signals: Applications to ECG Signals*, Proc.of IEEE signal processing society 10th DSP workshop, Georgia, 2002, pp.271-276.

[14] D.H.Mugler and S.Clary, *Discrete Hermite Functions and The Fractional Fourier Transform*, Proc. of Intn'l workshop on sampling theory, Orlando:SampTA'01, 2001,pp.303-308.

[15] D.H.Mugler and S.Clary, *Discrete Hermite Functions*, Processings of Int'l Conf. On Scientific computing and mathematical modeling,Milwaukee:IMACS, 2000, pp.318-321.

[16] D.H.Mugler, *Fast computation of the discrete Hermite transform*, (in preparation).

[17] D.H.Mugler AND S.Clary, *Shifted Fourier Matrices and Their Tridiagonal Commuters*, SIAM Journal on Matrix Analysis and Applications,24, 2003, pp.809-821.

[18] D.H.Mugler AND S.Clary, *Discrete Hermite Functions for DCT-4 and DST-4*,Private Communication.

[19] G.D.Bergland, *A Guided Tour of the Fast Fourier Transform*, IEEE Spectrum 6, July 1969, pp. 41-52.

[20] C.Papaloukas,. D.I.Fotiadis, A.Likas and L.K.Michalis, *Automated Methods for Ischemia Detection in Long Duration ECGs*, Cardiovasc Rev Rep, 24(6), pp. 313-320, 2003.

[21] C.Papaloukas, D.I.Dimitrios, A.Likas and L.K.Michalis, *An ischemic detection method based on artificial neural networks*, Artificial Intelligence in Medicine 24, 2002, pp. 167-178.

[22] I.Daskalov, I.Dotsinsky and I.Christov, *Developments in ECG Acquistion, Preprocessing, Parameter Measurement, and Recording*, IEEE Engineering in Medicine and Biology, March/April 1998, pp.50-58.

[23] T.Linh, S.Osowski AND M.Stodolski, *On-Line Heart Beat Recongnition Using Hermite Polynomials and Nuero-Fuzzy Network*, IEEE Transactions on Instrumentation and Measurement, 52 (4), August 2003, pp.1224-1231.

[24] J.Martens, *The Hermite Transform - Theory*, IEEE Transactions on Acoustics Speech and Signal Processing, 38 (9), September 1990, pp. 1595-1606.

[25] J.Martens, *The Hermite Transform - Applications*, IEEE Transactions on Acoustics Speech and Signal Processing, 38 (9), September 1990, pp. 1607-1618.

[26] G.Leibon, D.Rockmore, W.Park, R.Taintor and G.Chirikjian, *A fast Hermite Transform*, Theoretical Computer Science, 409, 2008, pp. 211-228.

[27] M.Lagerholm, C.Peterson, G.Braccini, L.Edenbr and L,Sornmo,*Clustering ECG Complexes Using Hermite Functions and Self-Organizing Maps*, IEEE Transactions on Biomedical Eng.,47 (7), 2000, pp.838-848.

[28] L.Wang, A.Bhalera AND R.Wilson, *Analysis of Retinal Vasculature Using a Multiresolution Hermite Model*, IEEE Trans Med Image, 26(2), pp. 137-152.

[29] M.Arichi, D.H.Mugler, *Fast Computation and Applications to Ischemic Detection from Electrocardiograms of the Dilated, Discrete Hermite Transform*,(in preparation).

[30] R. Rangayyan, *Biomedical Signal Analysis: A Case-Study Approach*, IEEE, Inc.,2002.

[31] H.S.Shin, C.Lee and M.Lee, *Principal Point Discrimination of Electrocardiogram for Automatic Diagnosis*, IFMBE Poceedings, Vol.14/2, Track 07, pp.1087-1090, 2007.

[32] I.K.Daskalov and I.I.Christov, *Automatic Detection of the Electrocardiogram T-wave end*, Med. Biol. Eng. Comput., Vol.37, pp.348-353, 1999.

[33] A.P. Engelbrecht, *Computational Intelligence: An Introduction*, John Wiley and Sons Ltd., 2002.